Journal of Ceramic Processing Research. Vol. 16, No. 5, pp. 536~540 (2015)

JOURNAL OF
Ceramic Processing Research

Fabrication and characterization of multi-layered ceramic ion generators based on dielectric barrier discharge

Hong-Je Choi[a,b], Byung-Ik Kim[a], Yong-Soo Cho[b] and Myoung-Pyo Chun[a,]*

[a]*Nano IT material team, Korea Institute of Ceramic Engineering and Technology (KICET), Jinju 52851, Korea*
[b]*Department of Materials Science and Engineering, Yonsei University, Seoul 120-749, Korea*

Multi-layered ceramic ion generators based on dielectric barrier discharge (DBD) were fabricated by a lamination process embedding the device with thick film patterns for applications of air purification and sterilization. The structure of the dielectric barrier discharge module consists of seven laminated Al_2O_3 layers containing top and inner conductor patterns functioning for the ion generators. The top layer of the laminated structure was passivated with MgO thick film of 20-30 μm for protection physically and electrically. Negative ions are generated on the top electrode layer with a sufficient applied voltage. Compared to a rectangular generator pattern, a radial pattern generated more negative ions by inducing electrons effectively around its sharp edges. The degree of negative ion generation was analyzed with two different top electrode patterns and different size of one of top patterns. The values of capacitance of the dielectric layer with respect to them. It was also observed that the appropriate magnitude of applied voltage was also very critical in determining enough ion generation without detrimental dielectric breakdown.

Key words: Dielectric barrier discharge, Multi-layer, Negative ion generator, Thick film, Electrode pattern.

Introduction

Dielectric barrier discharge (DBD), often known as silent discharge (SD) or partial discharge, has been commonly used in a number of broad applications, such as ozone reactor, SD CO_2 laser, air cleaner for vehicles and electronics, air contamination control, excimer UV sources, sterilization or bacterial inactivation, anionic dyeing and so on [1-11]. Among these DBD plasma methods, we focus on generating negative ions for healthy interior air condition. It has been considered that negatively charged ions are beneficial to the human body. They strengthen the functions of autonomic nerves, reinforce collagen and improve the permeability of the cell's prototype plasma membranes. Also, they strengthen the body's immune system [12, 13].

The DBD technique has been considerably attracted as one of the major plasma processes in the field of negative ion generation industries because of many advantages. As an advantageous example, harmful ozone can be less emitted and the discharge process is much simpler than other alternatives like electron beam, low pressure discharge and pulsed high pressure corona discharge. This cost-effective method can be operated at low temperatures and in atmospheric conditions without generating electrical shock [14,15]. However, there have been very limited studies on the fabrication process of the DBD based negative ion generators with multi-layered ceramic structure.

In dielectric barrier discharge, surface discharge appears on the top surface and the resultant energy outcome has a strong influence on the improvement of DBD efficiency [16]. In order to produce a great portion of negative ions, a proper top electrode pattern of the DBD module should be designed for better efficiency. Radial patterns with sharp edges with a few spikes, which is similar to the cathode structure of field emission display (FED), have been reported to be effective in gathering a plenty of negative ions [17, 18]. Generally, geometric structure of the electrode is very sensitive to overcome breakdown at high voltages [19-21]. An allowed maximum applied voltage that causes discharge without breakdown is ideal as related directly to electrical efficiency and lifetime extension [22].

In this research, the structural and physical properties of multi-layered ceramic ion generators based on the DBD phenomenon are investigated by comparing two different top electrode patterns with different pattern sizes. The number of generated negative ions is intimately associated with the operation condition as evidenced with experimental results. The approach of ceramic laminate specified for ion generators has not been reported so far.

Experimental Procedure

Multi-layered ceramic ion generators based on DBD were fabricated by tape casting combined with a thick

*Corresponding author:
Tel : +82-10-9080-1407
Fax: +82-55-792-2704
E-mail: myoungpyo@kicet.re.kr

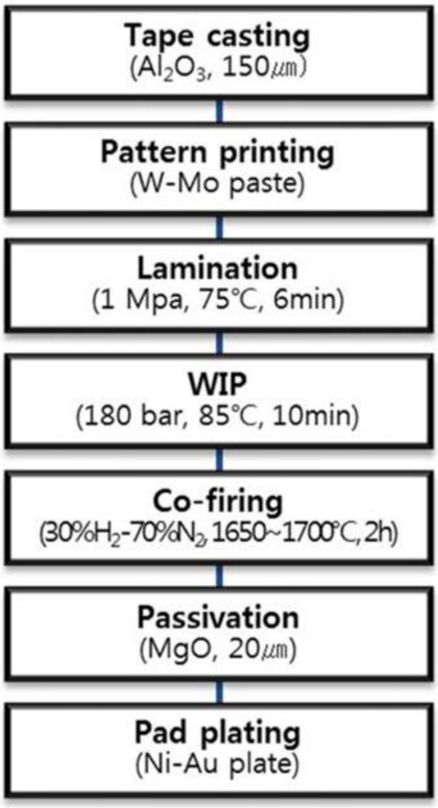

Fig. 1. Fabrication process of multi-layered ceramic ion generators based on DBD.

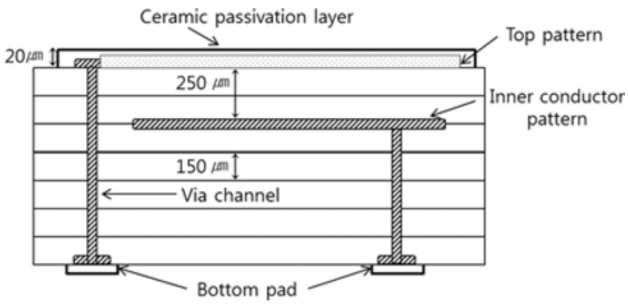

Fig. 2. Schematics of actual pattern designs: (a) top and (b) inner electrodes of the rectangular pattern, and (c) top and (d) inner electrodes of the radial pattern.

film printing process as shown in the flow chart of Fig. 1. High purity Al_2O_3 (99.9%, Sumitomo) was used as raw material for the individual sheet. A binder solution was made by dissolving PVB binder in a mixed solvent composed of ethanol and methyl ethyl ketone (MEK) for 24 h with alumina balls. Solid content, which is the relative weight of the Al_2O_3 ceramic powder to binder in slurry, is important for maintaining mechanical integrity during the handling of tapes. The proper chemistry of slurry may also help minimizing shrinkage difference between ceramic layers. The prepared slurry solution was tape-cast with the thickness of ~ 150 μm.

A W-Mo alloy paste was used for conductor electrodes. The top and inner electrode patterns were screen printed with the W-Mo paste onto the Al_2O_3 green sheet. Via holes connecting to the bottom terminal pads were formed by using a laser source and then filled with W-Mo by screen printing. Fig. 2 shows the cross-sectional schematic of the multi-layered ceramic negative ion generator. It consists of total seven Al_2O_3 layers with top and inner conductor layers. Via hole connections can be seen in this schematic. The thickness of dielectric layer between top and inner electrode was 250 μm, which affects the degree of ion discharge and the number of electrons accumulated on electrode surfaces.

The green sheets were first laminated under the uniaxial pressure of 1 MPa at 75 °C for 6 min and then isostatically pressed under 180 bar at 85 °C for 10 min. The laminate was singulated into an individual piece of the module by using a cutting machine. These pieces were co-fired in an electrical furnace in a reducing atmosphere of 30% H_2-70% N_2 at 1650 ~ 1700 °C for 2 h.

A paste of MgO (99.9%, High purity chemical) was printed as a passivation layer onto the top of fired module and then fired at 1530 °C. The thickness of the passivation layer was 20-30 μm. The passivation layer contributes to the stable operation of the module and thus the extension of the life time. Finally, terminal electrode pads as a bottom conductor in Fig. 2 were electro-plated with Ni.

In addition, we focused on how to make effective discharge because the number of emitted negative ions is proportional to the level of discharge. For understanding the relation of electrode pattern and discharge, the charge-voltage (Q-V) Lissajous diagram describing discharge energy and its factors was introduced [21]. Accordingly, the discharge energy W of DBD is given by

$$W = 4C_d V_0 \left(V_m - \frac{(C_a + C_d)}{C_d} V_0 \right)$$

where V_0 is the breakdown voltage, V_m is the maximum applied voltage. C_d is the capacitance of dielectric layer and C_a is the capacitance of air gap interior of the dielectrics. When we assume that V_m, V_0 and C_a are identical between patterns, only controllable factor is C_d in determining the final value of W. Since the thickness of each dielectric layer is also same, only the effective area of the pattern influences the performance of the ion generators because the value of capacitance is proportional to the overlap area of electrode pattern between top and inner layers. However, that area is not allowed to be extended until all of printed pattern area because of a chance of dielectric or electric breakdown. Thus, borders and a few spikes were considered as a proper top electrode design as shown in Fig. 3a and c. Inner electrode patterns of two different patterns were same as the top those but they were filled by printed conductors as depicted in Fig. 3b and d. We came up with two shapes of design as mentioned

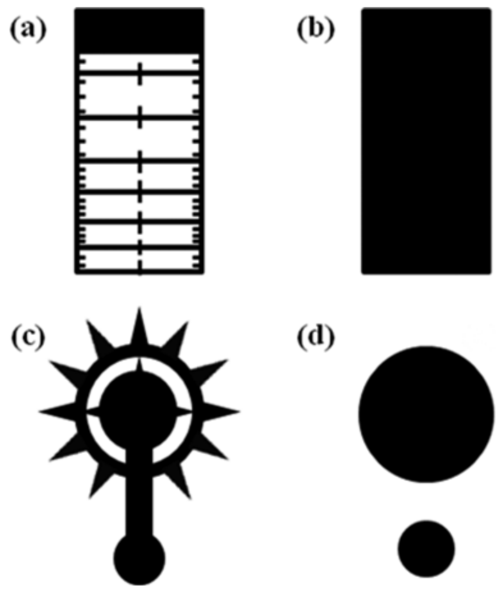

Fig. 3. Cross-sectional view of multi-layered ceramic structure for the negative ion generator.

Table 1. Dimensions of different top radial patterns.

Pattern size	Dimension (mm)
Small	7.5 × 11
Medium	10.5 × 15
Large	13.5 × 19

above. One is a rectangular pattern with spikes like Fig. 3a and another is a radial pattern with spikes around sharp edges as depicted in Fig. 3b. In order to figure out the influences of the size of electrode pattern on the negative ion generation, the devices composed of small, medium and large sized electrode patterns were fabricated. Table 1 shows the dimensional information of different radial array patterns.

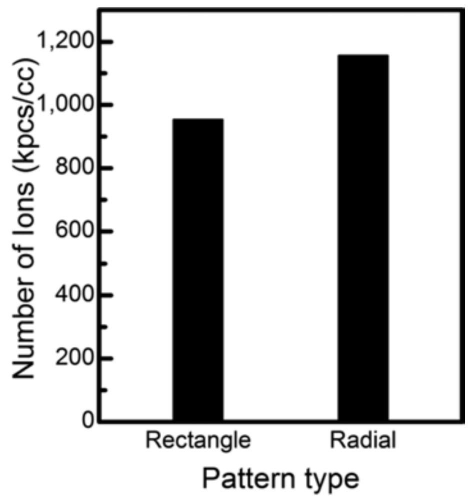

Fig. 4. The number of generated negative ions with the two different patterns.

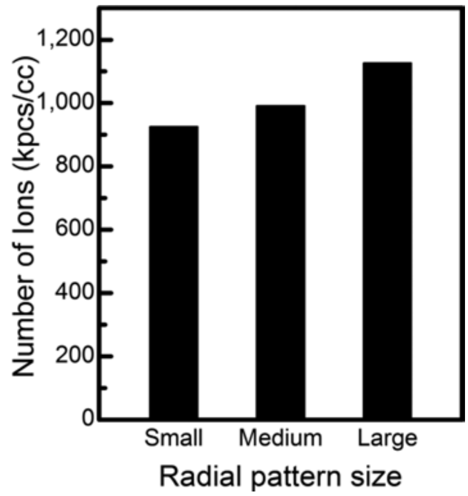

Fig. 5. The number of generated negative ions with different sizes of the radial pattern.

Results and Discussion

Fig. 4 shows the number of negative ions generated from the rectangular and radial patterns. The radial electrode pattern generated 1,156 kpcs per air of 1 cc while the rectangular electrode pattern emitted 954 kpcs/cc when 16 kV was applied. There is about 12% difference between the patterns. There are mainly two reasons why the number of generated ions depends on the type of pattern. There are two main different attributes between the rectangular and radial patterns: the number of spikes for emission and the overlap area between top and inner conductor layers. The rectangular pattern has only a few small spikes designed to attract electrons along with the pattern lines as shown in Fig. 3a. On the contrary, the radial pattern includes bigger spikes as shown in Fig. 3c. Basically, the working principle of spikes is similar to the role of cathode in of field emission devices. In field emission, a sufficiently high voltage generates electron emission at tips toward to anodes. The emitted electrons contribute to releasing more negative ions like discharge mechanism than when generated electrons by discharge participates only in making negative ions [19, 20]. Also, the current design of the radial pattern represents more electrode coverage area (or overlap area between top and inner conductors) and thus contributes to producing higher electron emission.

Fig. 5 shows the variations in the number of negative ions generated for three different sizes of the radial pattern making more negative ions as shown in Fig. 3c. As expected, a larger pattern resulted in a higher efficiency by showing a larger number of emitted ions. The small, medium and large patterns demonstrated values of 925 kpcs/cc, 991 kpcs/cc and 1,126 kpcs/cc, respectively. As estimated from the equations (1), the larger pattern leads to a higher value of C_d by providing more effective overlap emission area.

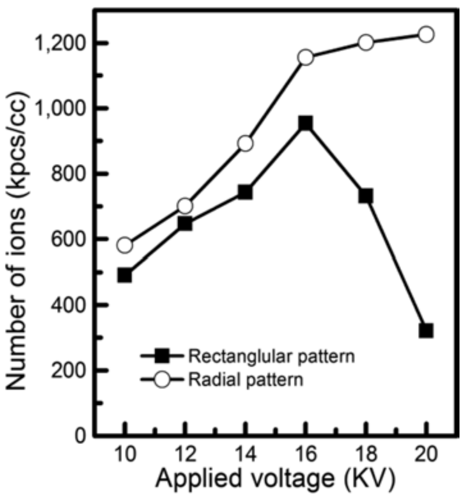

Fig. 6. Variations in the number of generated negative ions as a function of applied voltage for both patterns.

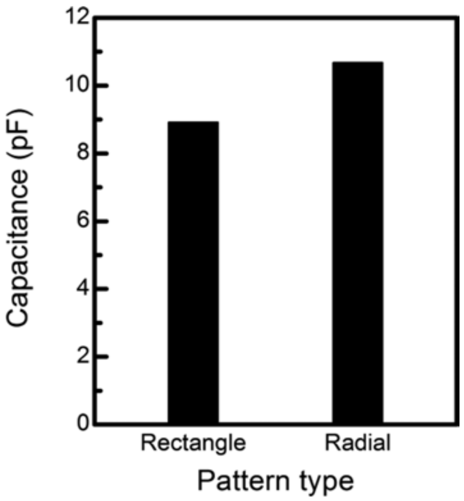

Fig. 7. Values of capacitance of the dielectric layer for both patterns.

Fig. 6 shows the plots of the number of generated negative ions with respect to increasing applied voltage for the two patterns to find the range of stable operation condition without breakdown. There are distinct differences between rectangular and radial top electrode patterns. The rectangular pattern had a peak of generated ions at 16 kV and then the rapid decrease with further increase in voltage. It is attributed to the initiation and progress of breakdown process as voltage is excessively applied. In comparison, the radial pattern showed the gradual increase of the ions within the voltage range up to 20 kV. Even, it releases more negative ions in the radial pattern than those of the rectangular pattern. Electric field is concentrated on sharp electrode pattern to facilitate the discharge of electrons near sharp electrodes. If electric field exceeds the critical value at local region, that region can be damaged partly due to dielectric breakdown induced by a high electric field. For the radial and rectangular top electrode patterns, radial pattern is more symmetric

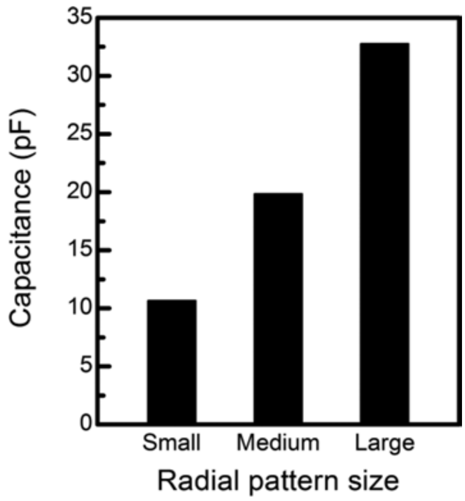

Fig. 8. Values of capacitance of the dielectric layer with different sizes of the radial pattern.

than rectangular one. So, electric field is more symmetrically distributed on the radial pattern than rectangular one. Therefore, at the same applied voltage, the maximum local electric field of the radical pattern seems to be lower than that of rectangular one, which means that the DBD of radial pattern will be damaged at the higher applied voltage than that of rectangular pattern and the number of generated negative ions with applied voltage increases up to higher range for the radial pattern than rectangular one due to a dielectric barrier layer less damaged.

We confirmed the changes of capacitance values according to the type of pattern and the size of the radial pattern. Fig. 7 and 8 shows the values of capacitance of the dielectric layer, which obtained between the top and inner conductor patterns. Again, the capacitance value of the dielectric depends on the effective overlap area between the electrode layers since the thickness of the identical Al_2O_3 dielectric layer is assumed to be same. Medium radial pattern produced more approximately 22% than medium rectangular pattern. As discussed earlier, the radial pattern with a largest pattern size demonstrated the highest value of 32.8 pF when 16 kV applied. This value is definitely responsible for the highest performance as ion generator. In conclusion, top electrode pattern of negative ion generators is very important for the enhancement of ion generation.

Conclusions

Multi-layered ceramic negative ion generators based on DBD were fabricated by the thick film technology. The design of the top layer electrode was found as a key parameter in obtaining the improved discharge efficiency indicating the availability of generated negative ions. The number of generated negative ions depended on the overlapped area between the top and inner electrode patterned layers because dielectric barrier discharge occurs between them. The number of spikes in the top pattern is also assumed to be important in generating more emissions from the device. The dependence of applied voltage to ion generation was confirmed before the excessive voltage produces unwanted electrical breakdown. The ceramic-based multilayer structure may be ideal in generating the negative ions since the design of various patterns can be applied and the ceramic itself has a very high breakdown voltage.

Acknowledgments

This work was supported by Seoul R&BD program (PA110044).

References

1. A. Warsito, A. Syakur, Syafrudin, G. Susilowati, Int. J. Elect. Comput. Eng. 1 (2011) 93-101.
2. L. Liu, J. Guo, J. Li, L. Sheng, J. Electrostatics 48 (2000) 81-91.
3. A. Bahrampour, A. Ganjovi, J. Phys. D : Appl. Phys. 36 (2003) 2487-2497.
4. Y. Zhang, J.H Mo, Y. Li, J. Sundell, P. Wargocki, J. Zhang, J. C. Little, R. Corsi, Q. Deng, M.H.K. Leung, L. Fang, W.Chen,J. Li, Y. Sun, Atmos. Environ. 45 (2011) 4329-4343.
5. X. Xu, Thin Solid Films 390 (2001) 237-242.
6. U. Kogelschatz, H. Esrom, J.-Y. Zhang, I.W. Boyd, Appl. Surface Sci, 168 (2000) 29-36.
7. U. Kogelschatz, B. Eliasson,W. Egli, Pure Appl. Chem., 71 (1999) 1819-1828.
8. U. Kogelschatz, Appl. Surf. Sci. 54 (1992) 410-423.
9. G. Fridman, A.D. Brooks, M. Balasubramanian, A. Fridman, A. Gutsol, V.N. Vasilets, H. Ayan, G. Friedman, Plasma Process. Polym. 4 (2007) 370-375.
10. A.P. Souto, Textile Dyeing (Intech, Winchester, 2011), p. 241-260.
11. T. Hammer, Contrib. Plasma Phys. 39 (1999) 441-462.
12. D.P. Uzunov, T.B. Cooper, E. Costa, A. Guidotti, Proc. Natl. Acad. 93 (1996) 12599-12604.
13. J.F. Hammerstone, S.A. Lazarus, A.E. Mitchell, R. Rucker, H.H. Schmitz, J. Agric. Food Chem. 47 (1999) 490-496.
14. U. Kogelschatz, B. Eliasson, W. Egli, J. Phys. IV France 7 (1997) C4-47.
15. G.H. Kim, S.H Song, J. Korean Physical Society 49 (2006) 558-562.
16. S. Liu, M. Neiger, J. Phys. D: Appl. Phys. 34 (2001) 1632-1638.
17. I. Kronhaus, A. Kapulkin, M. Guelman, J. Appl. Phys. 108 (2010) 054507.
18. Y. Liang, D.A. Bonnell, Appl. Phys. Lett. 66 (1995) 1147-1149.
19. U. Kogelschatz, Plasma Chem. and Plasma P. 23 (2003) 1-46.
20. Y.H. Kim, J.M. Park, S.H. Hong, J. Korean Physical Society 44 (2004) 1458-1467.
21. G.H. Kim, S.Y. Jeong, H.C. Kwon, J. Korean Physical Society 49 (2006) 1307-1311.
22. S.Z. Li, H.S. Uhm, J. Korean Physical Society 45 (2004) 409-415.